Backbone dynamics of the 8 kDa dynein light chain dimer reveals molecular basis of the protein's functional diversity

Jing-Song Fan, Qiang Zhang, Hidehito Tochio & Mingjie Zhang*
Department of Biochemistry, The Hong Kong University of Science and Technology, Clear Water Bay, Kowloon, Hong Kong, P.R. China

Abstract

Axonemal and cytoplasmic dyneins share a highly conserved 8 kDa light chain (DLC8) for motor assembly and function. Other than serving as a light chain of dynein complexes, DLC8 has been shown to bind a larger number of proteins with diverse biological functions including cell cycle control, apoptosis, and cell polarity maintenance. Therefore, DLC8 is likely a multifunctional regulatory protein. DLC8 exists as a dimer in solution, and the protein dimer is capable of binding to two target molecules. In this work, the backbone dynamics of DLC8, both in its apo- and target-peptide bound forms, were characterized by ^{15}N NMR relaxation studies. The relaxation data were analyzed using model-free approach. We show that the target peptide-binding region of apo-DLC8 experiences microsecond-to-millisecond time scale conformational fluctuation, suggesting that the target-binding region of the protein is capable of adjusting its shape and size in responding to its various targets. The conformational breathing of the target-binding region of apo-DLC8 was also supported by backbone amide exchange experiment. Such segmental conformational motion of the protein is significantly reduced upon forming a complex with a target peptide. The dynamic properties of DLC8 in solution provide insight into the protein's diverse sequence-dependent target binding.

Dyneins are microtubule-based molecular motors that provide forces for various motility processes in eukaryotic cells (Holzbaur and Vallee, 1994; Vallee and Sheetz, 1996; Hirokawa, 1998; King, 2000). The dynein superfamily proteins are divided into two major classes based on their distinct cellular functions. Cytoplasmic dyneins are involved in membrane-bound organelle transport, Golgi localization, spindle formation and orientation, nuclear localization and nucleic acid transport. Axonemal dyneins are largely responsible for providing motive force for ciliary and flagellar beating. All known dyneins contain multiple subunits, and the complexes have molecular masses of >1 MDa. Typically, each dynein contains two or three heavy chains each with molecular mass ~500 kDa (the globular heads of heavy chains contain ATPase

activity); two or more intermediate chains (MW, 70–80 kDa) that are apparently involved in attachment of the motor to some of its cargoes (King et al., 1991, 1995; Karki and Holzbaur, 1995; Vaughan and Vallee, 1995); and several light chains (MW, 8–22 kDa) of which the precise functions are still largely unknown (King and Patel-King, 1995a, b; King et al., 1996b; Patel-King et al., 1997; Pazour et al., 1999). Cytoplasmic dyneins also contain multiple copies of light intermediate chains that are distantly related to ABC transporters (Gill et al., 1994; Hughes et al., 1995).

The 8 kDa light chain of dynein (DLC8) is the smallest subunit in the motor complex. DLC8 was originally identified as a light chain of *Chlamydomonas* outer arm axonemal dynein (Piperno and Luck, 1979; King and Patel-King, 1995b). The protein was subsequently shown to be a component of cytoplasmic dyneins (King et al., 1996a) and *Chlamydomonas* inner arm dynein I1 (Harri-

son et al., 1998). The actual molecular weight of DLC8 is 10.3 kDa, but the protein migrates at 8 kDa on SDS-polyacrylamide gel electrophoresis. The protein has been highly conserved throughout evolution, with amino acid sequence identity of ∼90% in *Chlamydomonas, Caenorhabditis elegans, Drosophila melanogaster*, and human beings. Each cytoplasmic dynein contains two copies of DLC8, and the protein attaches itself to the motor via binding to the intermediate chains (Lo et al., 2001). Cellular fractionation of mammalian brain extracts revealed that only a minor fraction of DLC8 exists as a dynein-bound form, and the majority of the protein is not associated with microtubules (King et al., 1996a). The extremely high amino acid sequence conservation throughout evolution and the existence of multiple pools of the protein suggest that DLC8 may be involved in conserved functions in various biological processes. Indeed, a growing number of proteins have been identified as interacting with DLC8, and these DLC8-binding proteins are apparently involved in diverse biological processes. For example, the actin-based molecular motor myosin-V also binds to DLC8 in a stoichiometric manner (Espindola et al., 2000). In addition, DLC8 was found to specifically interact with neuronal nitric oxide synthase (Jaffrey and Snyder, 1996; Fan et al., 1998), transcriptional regulator IκB (Crepieux et al., 1997), proapoptotic Bcl-2 family protein Bim (Puthalakath et al., 1999), mRNA localization protein Swallow (Schnorrer et al., 2000), postsynaptic scaffold protein GKAP (Naisbitt et al., 2000), rabies virus phosphoprotein (Jacob et al., 2000; Raux et al., 2000), and nuclear respiratory factor-1 family transcription factors (Herzig et al., 2000). In *Drosophila*, partial mutation of DLC8 gene leads to defects in fly's bristle and wing development, female sterility, abnormal sensory axon projections; total loss of this protein is lethal due to apoptosis (Phillis et al., 1996; Dick et al., 1996). Mutation of DLC8 in *Aspergillus nidulans* inhibits nuclear migration (Beckwith et al., 1998). Deletion of DLC8 in *Chlamydomonas* leads to defects in flagellar ultrastructure and retrograde intraflagellar transport (Pazour et al., 1998). Disruption of the interaction between DLC8 and Swallow destroys the asymmetric distribution of Swallow protein in *Drosophila* (Schnorrer et al., 2000). DLC8 functions as a regulator of apoptosis by sequestering the proapoptotic protein Bim on microtubules via dynein complexes (Puthalakath et al., 1999). Only a subset of these DLC8-binding proteins contain 'K/R-X-T-Q-T' DLC8-binding motif (Lo et al., 2001), indicating

broad target recognition specificity of DLC8 (see Table 1 in Lo et al., 2001) for example). Structural studies showed that DLC8 uses the same binding grooves to interact with target peptides with entirely different amino acid sequences (Liang et al., 1999; Fan et al., 2001). The question of how DLC8 recognizes multiple targets with diverse amino acid sequences without compromising its interaction specificity and affinity therefore arises.

In this work, the backbone dynamics of DLC8 both in its apo- and target-peptide bound forms were characterized by ^{15}N-relaxation studies using NMR techniques. The data provide insights into the molecular mechanism of DLC8's multi-target recognition. Together with the 3D structures of the apo-protein and its complexes with target peptides, the molecular basis of DLC8's multifaceted functions is beginning to be uncovered.

Materials and methods

Sample preparations

Expression, purification and stable isotope labeling of rat DLC8 (the protein was also called PIN in these studies) were described in our earlier studies (Fan et al., 1998; Tochio et al., 1998). The 9-residue Bim peptide (MSCDKSTQT) comprises the DLC8-binding domain of amino acid residues 48–56 of Bim$_L$ (Puthalakath et al., 1999; Fan et al., 2001). The peptide was commercially synthesized and further purified by reverse-phase HPLC. A 1:1 (^{15}N-labeled DLC8:unlabeled peptide) DLC8 complex was prepared for backbone dynamic studies. All NMR samples were freshly dissolved in 100 mM potassium phosphate buffer, pH 7 containing 10 mM d_{10}-DTT. The concentration of NMR samples were ∼1.0 mM (measured as the monomer DLC8 concentration).

NMR spectroscopy

All NMR experiments were performed at 30 °C on a four-channel Varian Inova 500 MHz. NMR spectra were processed with the nmrPipe software package (Delaglio et al., 1995) and analyzed using PIPP (Garrett et al., 1991). The backbone chemical shift assignment of the apo-DLC8 and its complex with the Bim peptide were obtained as described elsewhere (Tochio et al., 1998; Fan et al., 2001).

The pulse sequences used to obtain the ^{15}N longitudinal relaxation times, T$_1$, the ^{15}N spin-spin re-

laxation times, T_2, and the ^{1}H-^{15}N steady-state NOE values were described previously (Farrow et al., 1994). The relaxation delays T for T_1 experiments were: 11.1, 88.8, 199.8, 333.0, 499.5, 710.4, 999.0, 1443.0 ms, and T for T_2 were: 16.3, 32.6, 48.9, 65.2, 81.5, 97.8, 114.1, 146.7 ms. A 450 μs delay between sequential ^{15}N pulses in the CPMG pulse train was employed to attenuate the ^{15}N signal loss during the T_2 relaxation period. Steady-state ^{1}H-^{15}N NOE values were determined at 500 MHz by recording spectra with and without a 3-second ^{1}H saturation prior to the start of the experiment. The total recycle delays for the NOE measurement with and without ^{1}H saturation were 4 and 7 sec, respectively. The recycle delays for ^{15}N T_1 and T_2 measurements were 2 s. A total of 32 transients were collected in the T_1, T_2 and NOE experiments. The steady state NOE values were determined from the ratios of the peak intensities with and without proton saturation. All of the spectra were recorded as 256 × 1024 (t_1 × t_2) complex data matrices. Lorentzian-to-Gaussian apodization functions were applied in both dimensions before Fourier transformation. All data were processed using nmrPipe and nmrDraw software (Delaglio et al., 1995), and peak intensities were characterized as volumes using surface fitting routines in the nmrPipe software. T_1 and T_2 values were obtained by non-linear least-square fitting of single exponential decays to the experimental data. The uncertainties of T_1 and T_2 values were estimated by Monte Carlo simulation as described in the literature (Palmer et al., 1991; Farrow et al., 1994). The relaxation data were analyzed by using the program Modelfree 4.0 (provided by A.G. Palmer). The selection criteria of the dynamic models followed those described earlier (Mandel et al., 1995; Tochio et al., 2000).

Results

DLC8 exists as a tight, symmetric dimer in solution (Fan et al., 2001). The protein contains two identical, elongated target-binding channels (Figure 1). The cross-over β2 strand (the β-strand involved in the three dimensional domain swapping of the protein dimer) forms the base of each channel. The amino acid residues from the β0, β3, the β2/β3 linker of the same subunit, and residues from the beginning of α2 in the neighboring subunit, form the peripherals of the channel. The base of each channel is largely hydrophobic, and the channel rim is surrounded by polar and charged residues (Fan et al., 2001). One end of the channel is relatively enriched with negatively charged residues, and the other end is more positively charged. To uncover the molecular basis of DLC8's multi-target recognition, we studied the backbone dynamics of the protein both in its apo- and target-peptide bound forms. We chose the DLC8-binding domain of Bim as DLC8's target as this peptide contains a 'K/R-X-T-Q-T'-motif (Lo et al., 2001). We have also studied the dynamics of DLC8 complexed with its binding domain of nNOS (which has a very different amino acid sequences, see Fan et al., 2001), and similar results were observed (data not shown).

^{15}N, T_1, T_2, NOE data of apo- and peptide-bound DLC8

The relaxation parameters (T_1, T_2, and NOE) of 79 out of a total of 89 residues were obtained for apo-DLC8 (Figure 2a–c). Of the 10 uncharacterized residues, the amides of Arg4 and Thr70, Tyr65 and Leu78 overlap in the 2D ^{1}H-^{15}N HSQC spectrum, Pro52 does not contain an amide proton; and the amides of Met1, Cys2, His72, Phe73 and Gln80 are too weak to obtain reliable data due to conformational exchange. The relaxation data for a total of 82 residues were measured for DLC8 in a complex with the Bim peptide (Figure 3a–c). Of the 7 uncharacterized residues, Met1 and Cys2 are too weak to be observed, Pro52 is not NMR observable, and the amides of Lys31 and Lys48, Q27 and Thr53 overlap. The 10% trimmed mean values (i.e., the relaxation parameters of those residues that are deviated more than 10% from the mean values are trimmed) of apo-DLC8 are 0.66 ± 0.03 s, 0.076 ± 0.006 s, 0.78 ± 0.03 and 8.69 ± 0.44 for T_1, T_2, NOE, and T_1/T_2, respectively. The corresponding T_1, T_2, NOE, and T_1/T_2 values for the DCL8/Bim peptide complex are 0.73 ± 0.02 sec, 0.071 ± 0.004 s, 0.76 ± 0.03 and 10.24 ± 0.56, respectively. The mean T_1/T_2 values of apo-DLC8 and the Bim peptide-bound protein were initially used to estimate the respective overall correlation times (τ_m) of the protein, and mean τ_m values of 10.72 ± 0.30 ns, and 11.84 ± 0.45 ns were obtained for apo-DLC8 and the peptide-bound form, respectively. The estimated τ_m values for apo-DLC8 and the peptide-bound form of the protein agree well with the dimeric structure of the protein in solution.
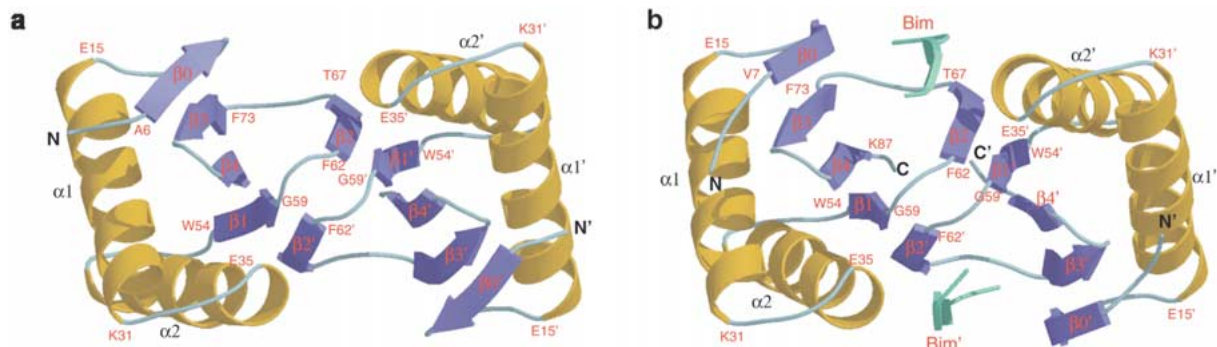
Figure 1. Ribbon diagram presentation of (a), the apo-DLC8 (PDB code 1F3C); and (b), its complex with the Bim peptide (PDB code 1F95). The secondary structure elements are labeled as described earlier (Fan et al., 2001). The starting and ending amino acid residues of each α-helix and β-strand are labeled with their names and numbers. The figure was generated using MOLSCRIPT (Kraulis, 1991) and Raster3D (Merritt and Murphy, 1994).
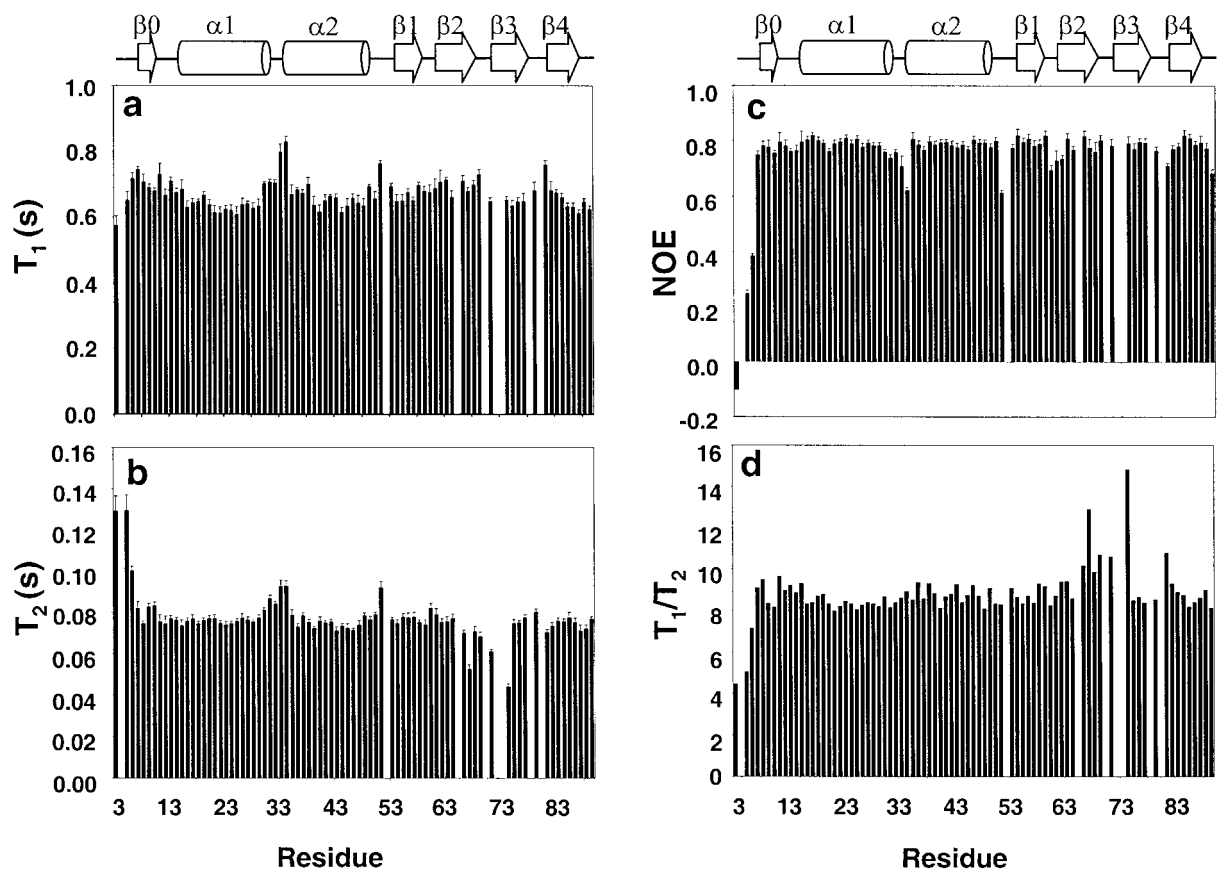

Figure 2. Plot as a function of amino acid residue number of measured (a), T_1, (b), T_2, (c), ^{1}H-^{15}N NOE, and (d), calculated T_1/T_2 ratios of apo-DLC8. The experimental errors in measuring T_1, T_2, and ^{1}H-^{15}N NOE values are also included in the figure. The secondary structure of the protein is shown on the top of the figure for easier correlation of each amino acid residue and its location in the structure of the protein.
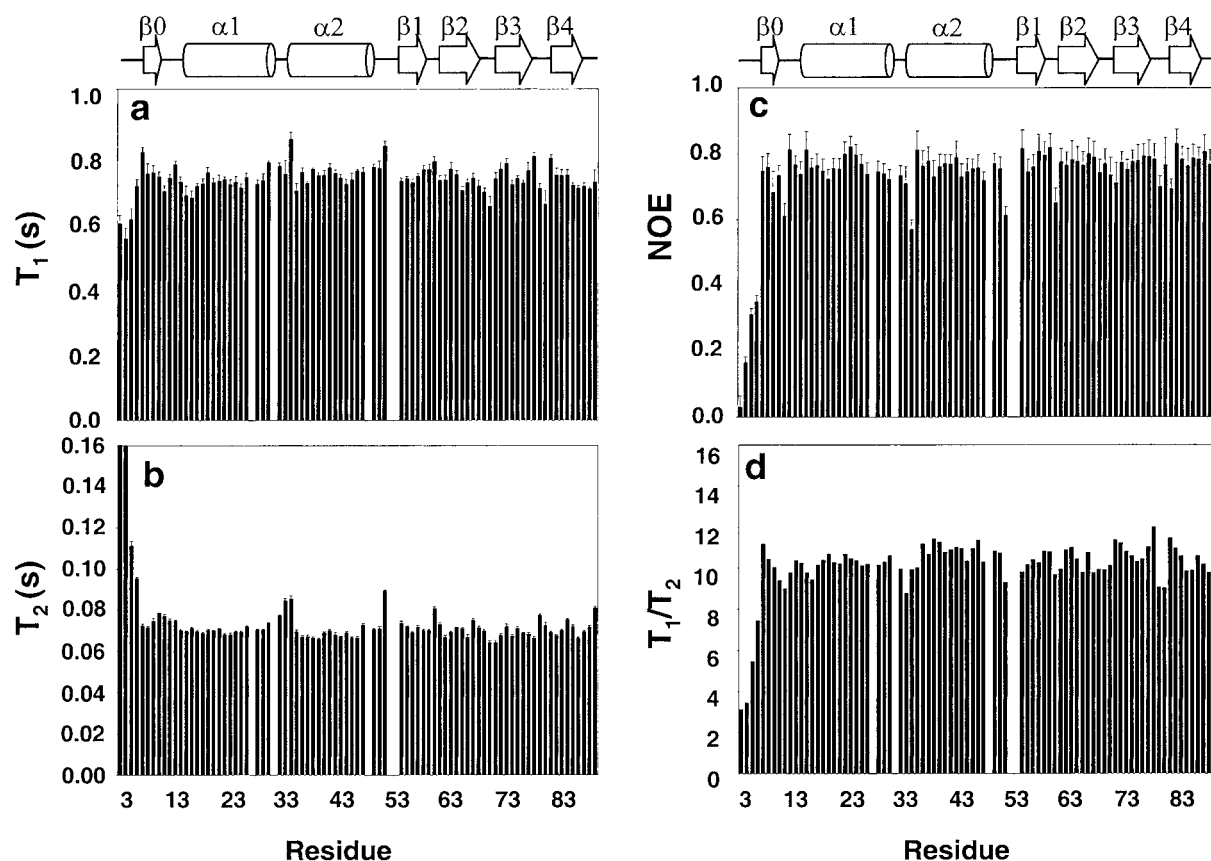
Figure 3. Plot as a function of amino acid residue number of measured (a), T_1, (b), T_2, (c), ^1H-^{15}N NOE, and (d), calculated T_1/T_2 ratios of DLC8 complexed with a short peptide encompassing the protein-binding domain of Bim.

Backbone dynamics of the apo- and the Bim peptide-bound forms of DLC8

The T_1, T_2, and NOE data were used to fit the extended Lipari-Szabo dynamic models following the methodology described by Mandel and co-workers (Lipari and Szabo, 1982a, b; Kay et al., 1989; Mandel et al., 1995). Since the structured regions of both apo- and the Bim peptide-bound forms of DLC8 are rather deviated from spherical shape in solution (the calculated principal axis ratios of 1.7:1.2:1.0 and 1.8:1.2:1.0 for the apo- and the peptide-bound forms of DLC8, respectively), we modeled the relaxation data of both forms of DLC8 using the axially symmetric, anisotropic tumbling model (Tjandra et al., 1995a; Lee et al., 1997), taking the solution structures of the protein dimer determined in our earlier studies (Fan et al., 2001). The $D_{//}/D_{\perp}$ asymmetric rotational diffusion ratios of 1.056 and 1.059 were obtained for the apo- and the Bim peptide bound DLC8, respectively, suggesting that DLC8 is not as asymmetric as indicated by the principal axis ratios calculated from the structural coordinates. It is possible that DLC8 may have an uneven hydration sphere on the surface of the protein. It is also possible that the majority of the N-H vectors in both apo-form and peptide-bound form of DLC8 are parallel to the long axis of the protein, such that these vectors do not sample most of orientations. We favor the latter as it is known to impact the analysis of relaxation data.

Five models were considered in fitting the relaxation data, which included: (1), S^2 only, τ_e and R_{ex} are negligible; (2), S^2 and τ_e only, R_{ex} is negligible; (3), S^2 and an R_{ex} term; (4), S^2, τ_e, and R_{ex}; and (5), incorporation of an additional order parameter for two time scale internal motions (S_f^2 and S_s^2 for internal motions on the fast and slow time scales). Figure 4a–c shows the fitted S^2, τ_e, and R_{ex} values for apo-DLC8. The fitted S^2, τ_e, and R_{ex} values of the Bim peptide-bound DLC8 are plotted in Figure 5a–c.
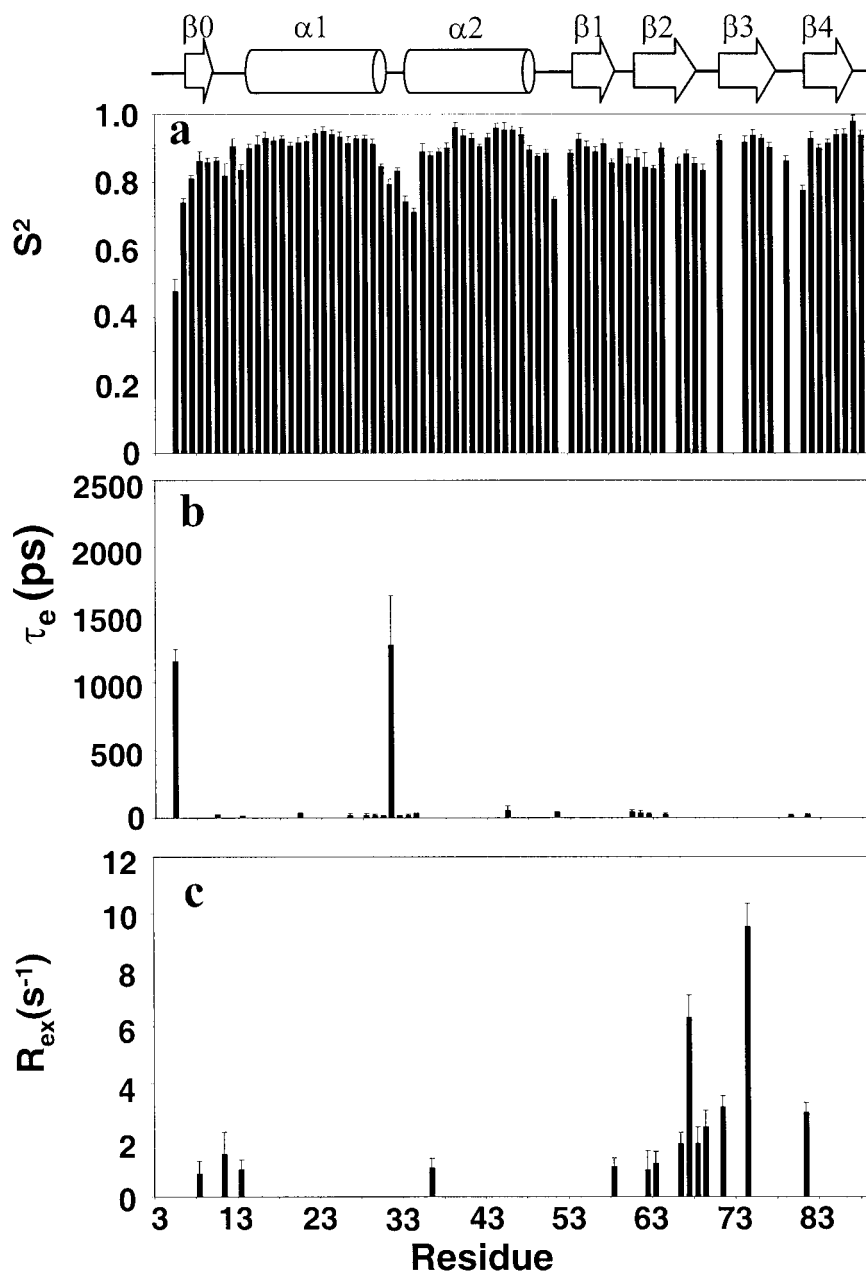
Figure 4. Results from the model-free analysis of apo-DLC8 are plotted as a function of amino acid sequence. (a), S^2; (b), τ_e; and (c) R_{ex}. The secondary structure of the protein is shown on the top of the figure for correlation of each amino acid residue number and its position in the 3D structure.

In general, the amino acid residues in the secondary-structured regions of apo-DLC8 have order parameters (S^2) of ~0.9, indicating that these regions behave rigidly in the picosecond-to-nanosecond time scale (Figure 4a). The residues at the amino terminus (residue 3–5) of the apo-protein have low S^2 and large τ_e values indicating fast motion in addition to the overall tumbling of the protein. The relaxation data for the N-terminal residues are consistent with the random coil structure of the protein in solution. The entire C-terminus of the protein is rigid as judged from the NOE values, consistent with significant amounts of medium- and long-range NOE contacts observed for the last two residues during

structural determination. The T_1/T_2 values for amino acid residues linking β2/β3 as well as at the end of β2 and the beginning of β3 (residues from Val66-Phe73) are significantly larger than the average value (Figure 2d). The amplitude of NOEs for this stretch of amino acids is rather close to the average value (Figure 2c). These amino acid residues need large R_{ex} values to fit their relaxation data, indicating that this contiguous stretch of peptide fragment experiences microsecond-to-millisecond time scale fluctuations. Such microsecond-to-millisecond time scale conformational exchange is also evidenced by the linewidth broadening of amide resonance in this region (the peak intensities of the residues His72, Phe73 and Gln80 were too weak to get reliable T2 data in the apo-protein). The observations of slow time scale conformational exchange of the β2/β3 loop, and the two flanking β-strands are further supported by the backbone amide exchange experiment (although amide exchange experiment is probing conformational exchange at a minutes-to-hours time scale). In apo-DLC8, the amide protons of the amino acids in the entire β2, the β2/β3 loop, and the beginning of β3 exchange rapidly with solvent Figure 6a, suggesting conformational breathing of the β2 and β3 strand. In addition, Val81 and several residues (Ile8, Ala11 and Met13) in the β0/α1 region also need an R_{ex} term to model their respective dynamic data. Figure 7a shows the spatial distribution of amino acid residues that require an R_{ex} term to fit their relaxation data. Upon inspection, it can be seen that these amino acid residues are clustered around the target peptide-binding channel of the protein.

As expected from the relatively small amplitude of target peptide-induced conformational changes (Fan et al., 2001), the overall backbone dynamics of DLC8 also remain largely unchanged upon binding to the Bim peptide, with the exception of the β2/β3 loop and part of β2 and β3 of the protein (Figures 4 and 5). The β2/β3 loop and part of β2 and β3 of the protein undergo slow time scale conformational fluctuations in apo-DLC8. In the complex, amino acid residues in these regions contact the target peptides directly (Fan et al., 2001). One can notice that the T_1/T_2 values of the amino acid residues in the regions are close to the average value of the protein. The relaxation data of the complex in these regions can be fitted with the exclusion of R_{ex} or with small R_{ex} values (< 2 Hz, which could be resulted from the experimental error in measuring original relaxation data), indicating that the conformational breathing of

this region of the DLC8/Bim peptide complex disappears/lessens (Figure 5). Backbone amide exchange experiments show that the entire β2 and β3 of DLC8 are protected from solvent exchange upon forming a complex with the Bim peptide (Figure 6b), further indicating that both β-strands have much lower degree of conformational fluctuation in the complex. The slower amide exchange rates of residues in the β2 and β3 are likely a combined result of more rigid conformation of the complex and the peptide-induced amide protection. The dynamic property changes of DLC8 resulting from binding to the Bim peptide are in parallel with the chemical shift changes of the protein induced by the same peptide (Figure 7b).

Discussion

Other than functioning as an essential subunit of dynein complexes, DLC8 interacts with a multitude of target proteins with diverse functions. The DLC8-binding domain of neuronal nitric oxide synthase has been mapped to a short stretch of amino acid residues (Fan et al., 1998; Liang et al., 1999). We further showed that a subset of DLC8-binding proteins contain a conserved 'K/R-X-T-Q-T'-motif (Lo et al., 2001). However, we were not able to find homologous amino acid sequences in other DLC8-binding proteins including nNOS, myosin V (Espindola et al., 2000; Naisbitt et al., 2000), GKAP (Naisbitt et al., 2000), Swallow (Schnorrer et al., 2000), and IκB (Crepieux et al., 1997), and NFR-1 (Herzig et al., 2000). Therefore, it is likely that DLC8 is able to bind to various targets with diverse amino acid sequences. Nevertheless, these proteins are likely to bind to DLC8 at an essentially identical manner (i.e., by pairing with the β2 strand of DLC8 in antiparallel fashion (Liang et al., 1999; Fan et al., 2001)). The interaction between DLC8 and its multiple targets is reminiscent of target recognition by calmodulin. The ubiquitous calcium signal modulator, calmodulin, was shown to interact with several dozens of target proteins. Like the binding domains of DLC8 targets, the calmodulin-binding domains (also contained within a short stretch of peptide fragment consisting of ~20 amino acid residues) of respective targets do not share obvious amino acid sequence homology. These calmodulin-binding peptides are able to bind to the same regions of calmodulin at an α-helical structure (for recent reviews, see Crivici and Ikura, 1995; Zhang and Yuan, 1998).
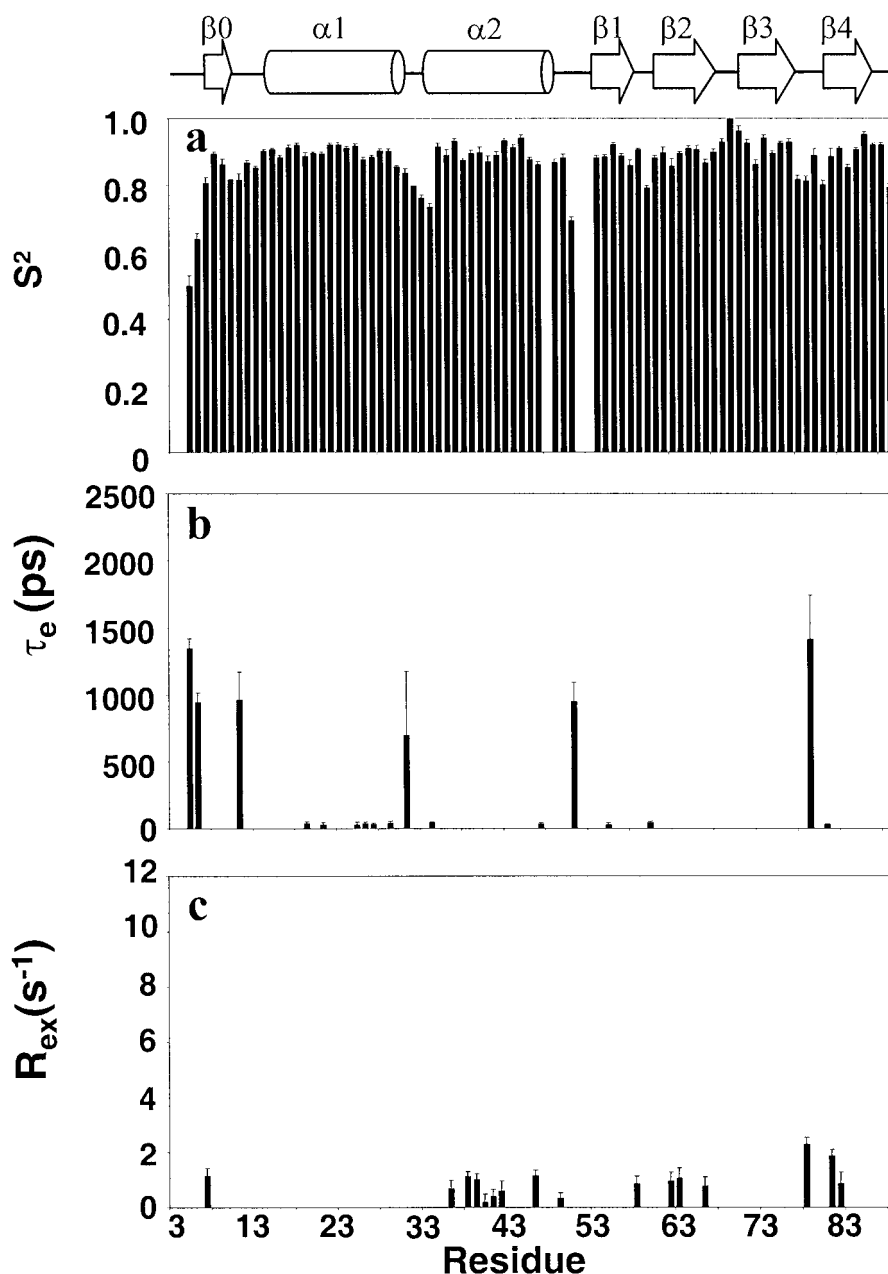
Figure 5. Results from the model-free analysis of DLC8/Bim peptide complex are plotted as a function of amino acid sequence. (a), S^2; (b), τ_e; and (c) R_{ex}.

In this work, we resorted to an analysis of the backbone dynamics of DLC8, both in its apo- and target-bound forms, to address its target recognition mechanism of the protein. The dimeric DLC8 has two identical, pre-formed channels, with one on each side of the dimer interface (Figure 1). The β2 strand in each channel serves as the template for incoming, ex-tended peptides. Two molecules of target peptides bind to DLC8 in an independent manner (data not shown). It is well known that formation of a β-sheet structure between two peptide backbones confers little speci-ficity. Therefore, specific target recognition by DLC8 has to involve interactions beyond the backbones of the protein and the target peptides. The structure of
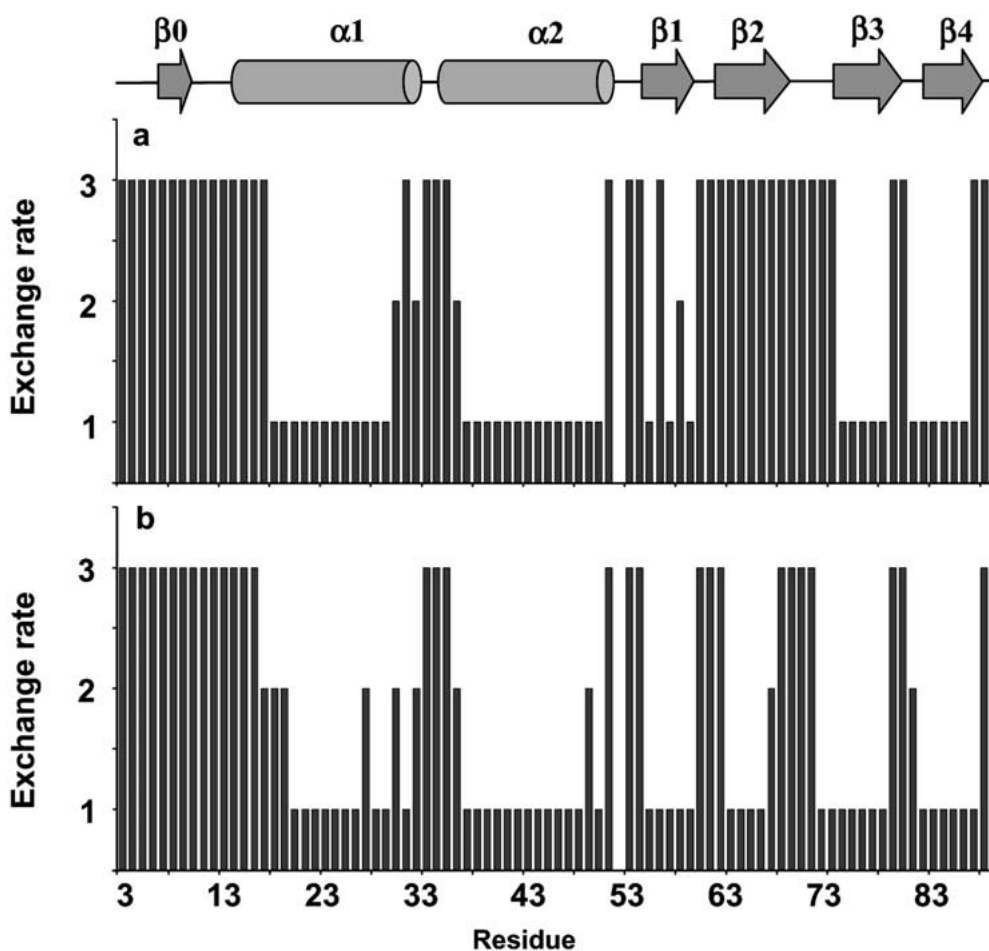
Figure 6. Backbone amide exchange rates of apo-DLC8 (a) and the Bim peptide-bound protein (b) determined by amide exchange-out experiments. The amide exchange rates of amino acid residues in both forms of DLC8 are categorized into three classes. The amides of the residues that immediately disappeared upon dissolving ^{15}N-labelled, protonated protein samples in D_2O buffer are classified as fast-exchanging amides (with an arbitrary scale of '3'). The amides that were observable after dissolving in D_2O buffer, but which disappeared within ~120 min after dissolution, are assigned as having medium-exchange rates (a scale of '2'). Finally, the amides that were protected from exchange ~120 min after dissolving in D_2O buffer are termed slow-exchanging amides (a scale of '1'). The amide resonances that overlap with each other and Pro52 are assigned a value of '0'.

the apo-DLC8 shows that the relatively hydrophobic base of the binding channel (the β2 strand) is surrounded by discretely-distributed polar and charged amino acid residues (Fan et al., 2001). In particular, the highly conserved, polar amino acid residues in the β2/β3 loop, Asp12 in the β0/α1 loop, and Glu35 and Lys36 at the beginning of the α2 helix were found to play critical roles in binding to target peptides (Fan et al., 2001). Of particular interest is the correlation between the dynamics of the protein and its multiple target-binding properties. A striking overlap can be observed between the regions of the protein exhibiting significant motions (residues that need R_{ex} to model dynamic data) and those

in direct contact with target peptides (Figure 7). In apo-DLC8, the target-accepting β2-strand and its C-terminal loop experience microsecond-to-millisecond conformational fluctuation. The conformational flexibility of the peptide-binding channels is likely to play an important role in the interaction of DLC8 with its multiple targets containing diverse recognition sequences. It is conceivable that peptides with different amino acid sequences have various shapes and charge properties, and DLC8 may employ different amino acid side-chains in its target-binding region to interact with its targets. Formation of specific, high affinity complexes between DLC8 and its target peptides will require the peptide-binding chan-
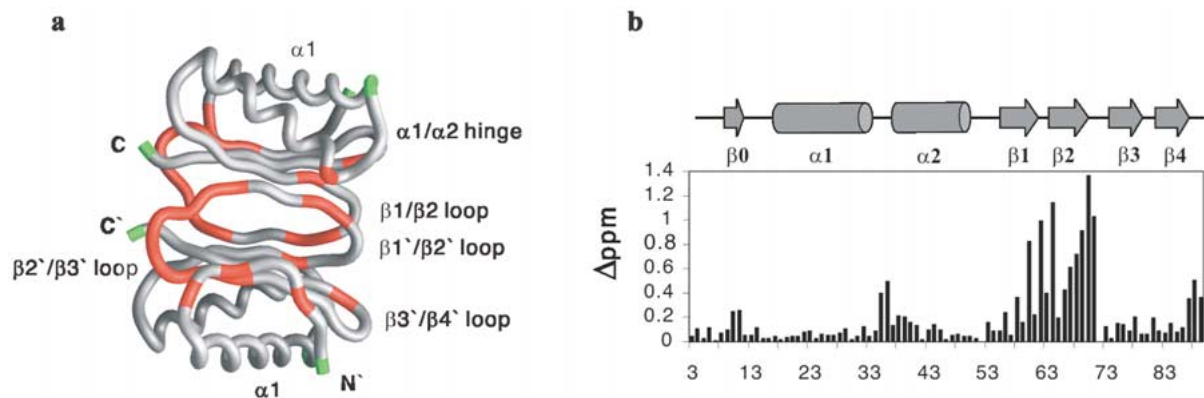
Figure 7. Correlating dynamic motion and chemical shifts with the target-binding of DLC8. (a) The amino acid residues of apo-DLC8 that have significant microsecond-to-millisecond time scale fluctuations, R_{ex}, are drawn in red, and the amino acid residues that need τ_e values (greater than 500 ps) to fit their relaxation data are drawn in green. The partial secondary structural elements of the protein are labeled. (b) Combined chemical shift changes of DLC8 resulted from the Bim peptide binding. The chemical shift changes are defined as: $\Delta_{ppm} = \sqrt{(\Delta\delta_{HN})^2 + (\Delta\delta_N * \alpha_N)^2}$. The scaling factor ($\alpha_N$) used to normalize the ^{1}H and ^{15}N chemical shifts is 0.17. The secondary structure of DLC8 is shown at the top of the figure.

nel to adjust its shape and size. For example, the DLC8-binding domain of nNOS is more bulky than the DLC8-binding domain of Bim (Fan et al., 2001). The hydrophobic interactions between the side chains of nNOS and DLC8 play an important role in the complex formation, whereas, the side-chain interactions between DLC8 and Bim are primarily mediated by charge-charge and hydrogen-bonding interactions (Fan et al., 2001). The intrinsic conformational flexibility of DLC8's target-binding channel is likely to facilitate the necessary size and shape changes in order to accommodate various targets. Likewise, it has been shown that the conformational flexibility of the peptide-binding surface plays a critical role in calmodulin's multi-target recognition (Zhang et al., 1994). Upon binding to the Bim peptide, the conformational flexibility of the peptide-binding channel is significantly reduced. In particular, both dynamic data and amide exchange results show that the entire β2 strand loses its slow time scale conformational fluctuations. Similar protein-peptide, protein-protein, and protein-DNA binding-induced conformation transitions from a relatively disordered free form to more ordered conformations in their respective complex forms have been observed (Kriwacki et al., 1996; Gryk et al., 1996; Wyss et al., 1997; Feher and Cavanagh, 1999). Such conformational flexibility has been shown to often play important roles for regulatory proteins. One can envision that such conformational flexibility allows regulatory proteins to sense their respective cues (various ligands including proteins, nucleic acids, car-

bohydrates and metal ions). Decreases of conformational flexibility upon formation of complexes with their respective ligands are likely to correlate with the completion of the signal sensing of these proteins. Although disordered-to-ordered conformational transition, accompanied by macromolecular complex formation, is likely a common observation, a decrease in conformational flexibility does not have to be a prerequisite for productive complex formation between two macromolecules. In contrast, an increase in dynamical flexibility can also occur in protein-ligand complex formation (Kay et al., 1998; Zidek et al., 1999). Perhaps one should not expect a simple rule that governs the dynamic properties of proteins as they are designed to carry out a wide spectrum of biological functions in living cells.

We note that the amino acid residues in the α1/α2 loop of DLC8 remain flexible after the protein forms a complex with the Bim peptide. The flexibility of the α1/α2 loop may be important for DLC8 to interact with its targets. The amino acid residues in this loop are not directly involved in target binding. However, the first two amino acid residues in the α2 helix (Glu35 and Lys36) play important roles in target binding (Fan et al., 2001). Upon forming a complex with the Bim peptide, the α2 helix changes its orientation, and conformational flexibility of the α1/α2 loop is likely to support such segmental helix motion. By analogy, the flexible amino acid residues connecting the two domains of calmodulin play critical roles in permitting the two domains of calmodulin to adopt various ori-

entations necessary for target peptides with different lengths, although the amino acid residues in the linker region do not contact directly with target peptides (Meador et al., 1993; Tjandra et al., 1995b).

It is important to note that although the dynamic studies have provided a correlation between the structural features of the protein and its target-binding capacity, further work is necessary to establish the function of the dynamic flexibility of DLC8 and its multi-target binding capacity. Extensive site-directed mutagenesis and chemical cross-linking studies have been initiated to assess the functional significance of the slow time scale conformational exchange observed in this study.

Acknowledgements

References

Beckwith, S.M., Roghi, C.H., Liu, B. and Ronald Morris, N. (1998) *J. Cell. Biol.*, **143**, 1239–1247.

Crepieux, P., Kwon, H., Leclerc, N., Spencer, W., Richard, S., Lin, R. and Hiscott, J. (1997) *Mol. Cell. Biol.*, **17**, 7375–7385.

Crivici, A. and Ikura, M. (1995) *Annu. Rev. Biophys. Biomol. Struct.*, **24**, 85–116.

Delaglio, F., Grzesiek, S., Vuister, G.W., Zhu, G., Pfeifer, J. and Bax, A. (1995) *J. Biomol. NMR*, **6**, 277–293.

Dick, T., Ray, K., Salz, H.K. and Chia, W. (1996) *Mol. Cell. Biol.*, **16**, 1966–1977.

Espindola, F.S., Suter, D.M., Partata, L.B., Cao, T., Wolenski, J.S., Cheney, R.E., King, S.M. and Mooseker, M.S. (2000) *Cell Motil. Cytoskeleton*, **47**, 269–281.

Fan, J.S., Zhang, Q., Li, M., Tochio, H., Yamazaki, T., Shimizu, M. and Zhang, M. (1998) *J. Biol. Chem.*, **273**, 33472–33481.

Fan, J.S., Zhang, Q., Tochio, H., Li, M. and Zhang, M. (2001) *J. Mol. Biol.*, **306**, 97–108.

Farrow, N.A., Muhandiram, R., Singer, A.U., Pascal, S.M., Kay, C.M., Gish, G., Shoelson, S.E., Pawson, T., Forman-Kay, J.D. and Kay, L.E. (1994) *Biochemistry*, **33**, 5984–6003.

Feher, V.A. and Cavanagh, J. (1999) *Nature*, **400**, 289–293.

Garrett, D.S., Powers, R., Gronenborn, A.M. and Clore, G.M. (1991) *J. Magn. Reson.*, **95**, 214–220.

Gill, S.R., Cleveland, D.W. and Schroer, T.A. (1994) *Mol. Biol. Cell*, **5**, 645–654.

Gryk, M.R., Jardetzky, O., Klig, L.S. and Yanofsky, C. (1996) *Protein Sci.*, **5**, 1195–1197.

Harrison, A., Olds-Clarke, P. and King, S.M. (1998) *J. Cell. Biol.*, **140**, 1137–1147.

Herzig, R.P., Andersson, U. and Scarpulla, R.C. (2000) *J. Cell. Sci.*, **113**, 4263–4273.

Hirokawa, N. (1998) *Science*, **279**, 519–526.

Holzbaur, E.L. and Vallee, R.B. (1994) *Annu. Rev. Cell Biol.*, **10**, 339–372.

Hughes, S.M., Vaughan, K.T., Herskovits, J.S. and Vallee, R.B. (1995) *J. Cell. Sci.*, **108**, 17–24.

Jacob, Y., Badrane, H., Ceccaldi, P.E. and Tordo, N. (2000) *J. Virol.*, **74**, 10217–10222.

Jaffrey, S.R. and Snyder, S.H. (1996) *Science*, **274**, 774–777.

Karki, S. and Holzbaur, E.L. (1995) *J. Biol. Chem.*, **270**, 28806–28811.

Kay, L.E., Muhandiram, D.R., Wolf, G., Shoelson, S.E. and Forman-Kay, J.D. (1998) *Nat. Struct. Biol.*, **5**, 156–163.

Kay, L.E., Torchia, D.A. and Bax, A. (1989) *Biochemistry*, **28**, 8972–8979.

King, S.M. (2000) *Biochim. Biophys. Acta*, **1496**, 60–75.

King, S.M., Barbarese, E., Dillman, III, J.F., Patel-King, R.S., Carson, J.H. and Pfister, K.K. (1996a) *J. Biol. Chem.*, **271**, 19358–19366.

King, S.M., Dillman, III, J.F., Benashski, S.E., Lye, R.J., Patel-King, R.S. and Pfister, K.K. (1996b) *J. Biol. Chem.*, **271**, 32281–32287.

King, S.M. and Patel-King, R.S. (1995a) *J. Cell. Sci.*, **108**, 3757–3764.

King, S.M. and Patel-King, R.S. (1995b) *J. Biol. Chem.*, **270**, 11445–11452.

King, S.M., Patel-King, R.S., Wilkerson, C.G. and Witman, G.B. (1995) *J. Cell. Biol.*, **131**, 399-409.

King, S.M., Wilkerson, C.G. and Witman, G.B. (1991) *J. Biol. Chem.*, **266**, 8401–8407.

Kraulis, P.J. (1991) *J. Appl. Crystallogr.*, **24**, 946–950.

Kriwacki, R.W., Hengst, L., Tennant, L., Reed, S.I. and Wright, P.E. (1996) *Proc. Natl. Acad. Sci. USA*, **93**, 11504–11509.

Lee, L.K., Rance, M., Chazin, W.J. and Palmer, III, A.G. (1997) *J. Biomol. NMR*, **9**, 287–298.

Liang, J., Jaffrey, S.R., Guo, W., Snyder, S.H. and Clardy, J. (1999) *Nat. Struct. Biol.*, **6**, 735–740.

Lipari, G. and Szabo, A. (1982a) *J. Am. Chem. Soc.*, **104**, 4546–4559.

Lipari, G. and Szabo, A. (1982b) *J. Am. Chem. Soc.*, **104**, 4559–4570.

Lo, K.W., Naisbitt, S., Fan, J.S., Sheng, M. and Zhang, M. (2001) *J. Biol. Chem.*, **276**, 14059–14066.

Mandel, A.M., Akke, M. and Palmer, III, A.G. (1995) *J. Mol. Biol.*, **246**, 144–163.

Meador, W.E., Means, A.R. and Quiocho, F.A. (1993) *Science*, **262**, 1718–1721.

Merritt, E. and Murphy, M. (1994) *Acta. Cryst.*, **D50**, 869–873.

Naisbitt, S., Valtschanoff, J., Allison, D.W., Sala, C., Kim, E., Craig, A. M., Weinberg, R.J. and Sheng, M. (2000) *J. Neurosci.*, **20**, 4524–4534.

Palmer, III, A.G., Rance, M. and Wright, P.E. (1991) *J. Am. Chem. Soc.*, **113**, 4371–4380.

Patel-King, R.S., Benashski, S.E., Harrison, A. and King, S.M. (1997) *J. Cell. Biol.*, **137**, 1081–1090.

Pazour, G.J., Koutoulis, A., Benashski, S.E., Dickert, B.L., Sheng, H., Patel-King, R.S., King, S.M. and Witman, G.B. (1999) *Mol. Biol. Cell*, **10**, 3507–3520.

Pazour, G.J., Wilkerson, C.G. and Witman, G.B. (1998) *J. Cell Biol.*, **141**, 979–992.

Phillis, R., Statton, D., Caruccio, P. and Murphey, R.K. (1996) *Development*, **122**, 2955–2963.

Piperno, G. and Luck, D.J. (1979) *J. Biol. Chem.*, **254**, 3084–3090.

Puthalakath, H., Huang, D.C., O'Reilly, L.A., King, S.M. and Strasser, A. (1999) *Mol. Cell*, **3**, 287–296.

Raux, H., Flamand, A. and Blondel, D. (2000) *J. Virol.*, **74**, 10212–10216.

Schnorrer, F., Bohmann, K. and Nusslein-Volhard, C. (2000) *Nat. Cell. Biol.*, **2**, 185–190.

Tjandra, N., Feller, S.E., Pastor, R.W. and Bax, A. (1995a) *J. Am. Chem. Soc.*, **117**, 12562–12566.

Tjandra, N., Kuboniwa, H., Ren, H. and Bax, A. (1995b) *Eur. J. Biochem.*, **230**, 1014–1024.

Tochio, H., Hung, F., Li, M., Bredt, D.S. and Zhang, M. (2000) *J. Mol. Biol.*, **295**, 225–237.

Tochio, H., Ohki, S., Zhang, Q., Li, M. and Zhang, M. (1998) *Nat. Struct. Biol.*, **5**, 965–969.

Vallee, R.B. and Sheetz, M.P. (1996) *Science*, **271**, 1539–1544.

Vaughan, K.T. and Vallee, R.B. (1995) *J. Cell Biol.*, **131**, 1507–1516.

Wyss, D.F., Dayie, K.T. and Wagner, G. (1997) *Protein Sci.*, **6**, 534–542.

Zhang, M., Li, M., Wang, J.H. and Vogel, H.J. (1994) *J. Biol. Chem.*, **269**, 15546–15552.

Zhang, M. and Yuan, T. (1998) *Biochem. Cell. Biol.*, **76**, 313–323.

Zidek, L., Novotny, M.V. and Stone, M.J. (1999) *Nat. Struct. Biol.*, **6**, 1118–11121.